

Deprotonation of $\eta^2(4e)$ -Bonded Alkynes as a Pathway to $\sigma, \eta^2(3e)$ -Prop-2-ynyl, η^5 -Pentadienyl and η^4 -*trans*-1,3-Diene Substituted Molybdenum Complexes *

Carla Carfagna,^a Robert J. Deeth,^a Michael Green,^{a,b} Mary F. Mahon,^a Jacqueline M. McInnes,^a Sylvan Pellegrini^a and Christopher B. Woolhouse^b

^a School of Chemistry, University of Bath, Claverton Down, Bath BA2 7AY, UK

^b Department of Chemistry, King's College London, Strand, London WC2R 2LS, UK

Addition of $\text{Li}[\text{N}(\text{SiMe}_3)_2]$ to the halogenobis(alkyne) complexes $[\text{MoBr}(\eta^2\text{-MeC}_2\text{R})_2(\eta\text{-C}_5\text{H}_5)]$ ($\text{R} = \text{Me}$ or Ph) resulted in a dehydrohalogenation reaction and formation of the $\sigma, \eta^2(3e)$ -prop-2-ynyl/ $\eta^2(4e)$ -alkyne-substituted complexes $[\text{Mo}\{\sigma, \eta^2(3e)\text{-CH}_2\text{C}_2\text{R}\}\{\eta^2(4e)\text{-MeC}_2\text{R}\}(\eta\text{-C}_5\text{H}_5)]$ ($\text{R} = \text{Ph}$ **7** or Me). The structure when $\text{R} = \text{Ph}$ has been confirmed by a single-crystal X-ray diffraction study. The $\eta^2(4e)$ -bonded alkyne and $\sigma, \eta^2(3e)$ -prop-2-ynyl ligands lie in planes essentially parallel to that of the $\eta\text{-C}_5\text{H}_5$ ligand, with a $\text{C}(1)\text{-C}(2)\text{-C}(3)$ angle and $\text{Mo-C}(1)$, $\text{Mo-C}(2)$ and $\text{Mo-C}(3)$ bond lengths for the prop-2-ynyl fragment of $146.1(6)^\circ$, $2.278(6)$, $2.164(5)$ and $2.105(5)$ Å respectively. The nature of the $\text{M}-\sigma, \eta^2\text{-C}_3\text{H}_3$ bonding in complex **7** and in the related species $[\text{Mo}\{\sigma, \eta^2(3e)\text{-CH}_2\text{C}_2\text{H}\}(\text{CO})_2(\eta^5\text{-C}_5\text{Me}_5)][\text{BF}_4]$ and $[\text{ZrMe}\{\sigma, \eta^2(3e)\text{-CH}_2\text{C}_2\text{Ph}\}(\eta\text{-C}_5\text{H}_5)_2]$ has been examined using a comparative standard extended-Hückel molecular orbital (EHMO) study. Reprotonation of the new complexes with $\text{CF}_3\text{CO}_2\text{H}$ affords $[\text{Mo}(\text{O}_2\text{CCF}_3)(\eta^2\text{-MeC}_2\text{R})_2(\eta\text{-C}_5\text{H}_5)]$ ($\text{R} = \text{Ph}$ or Me), and it is suggested in agreement with an EHMO charge-distribution calculation that protonation occurs initially on an alkyne contact carbon followed by transfer of the hydrogen *via* the metal to the prop-2-ynyl ligand. An attempt to extend the deprotonation reaction to the X-ray crystallographically identified η^2 -alkene/ $\eta^2(4e)$ -alkyne-substituted complex $[\text{Mo}\{\eta^2(4e)\text{-MeC}_2\text{Ph}\}(\text{dppe})(\eta\text{-C}_5\text{H}_5)][\text{BF}_4]$ ($\text{dppe} = o$ -diphenylphosphinostyrene) resulted in an unexpected reaction. Treatment with $\text{Li}[\text{N}(\text{SiMe}_3)_2]$ afforded the η^5 -pentadienyl complex $[\text{Mo}\{\eta^2, \eta^3(5e)\text{-CH}_2\text{CHC}(\text{Ph})\text{CH}=\text{CHC}_6\text{H}_4\text{PPh}_2\text{-}o\}(\eta\text{-C}_5\text{H}_5)]$, which was structurally characterised by single-crystal X-ray crystallography. The pentadienyl ligand is wrapped around the molybdenum atom resulting in a dihedral angle of 122° for $\text{C}(27)\text{-C}(26)\text{-C}(25)\text{-C}(24)$. The bond length $\text{C}(25)\text{-C}(26)$ of $1.484(11)$ Å indicates there is little interaction between the η^3 and η^2 π systems. Reaction of this complex with $\text{HBF}_4\cdot\text{Et}_2\text{O}$ resulted in the formation of a cationic *trans* (twisted) η^4 -1,3-diene substituted complex stabilised by an $\text{Mo}(\mu\text{-H})\text{C}$ interaction. A single-crystal X-ray diffraction study confirmed these features. The *trans*-1,3-diene carbons adopt a twisted, non-planar arrangement with a dihedral angle of 123° . The agostic interaction is not displaced by carbon monoxide.

We have previously^{1,2} reported that addition of NEt_3 to a solution of the $\eta^2(4e)$ -donor alkyne complex $[\text{Mo}(\eta^2\text{-PhC}_2\text{CH}_2\text{Ph})\{\text{P}(\text{OMe})_3\}_2(\eta\text{-C}_5\text{H}_5)][\text{BF}_4]$ **1** in $(\text{CD}_3)_2\text{CO}$ results in selective deuteration of the benzylic hydrogens. This suggested that irreversible deprotonation of this complex might lead to a novel reaction. Indeed treatment of **1** with $\text{KH-Bu}^t\text{-OH-Et}_2\text{O}$ results in loss of H_2 and formation of the isomeric $\eta^2(3e)$ -allenyl complexes $[\text{Mo}\{\text{C}(\text{Ph})\text{C}=\text{C}(\text{H})\text{Ph}\}\{\text{P}(\text{OMe})_3\}_2(\eta\text{-C}_5\text{H}_5)]$ **2** and $[\text{Mo}\{\text{C}(\text{Ph})\text{C}=\text{C}(\text{Ph})\text{H}\}\{\text{P}(\text{OMe})_3\}_2(\eta\text{-C}_5\text{H}_5)]$ **3**. In a related study reported by Templeton and co-workers³ it was shown that deprotonation of $[\text{W}(\text{S}_2\text{-CNR}_2)(\eta^2\text{-MeOC}_2\text{CH}_2\text{Ph})(\text{CO})(\text{dppe})][\text{X}]$ [$\text{dppe} = (\text{Ph}_2\text{-PCH}_2)_2$; $\text{R} = \text{Me}$ or Pr^i , $\text{X} = \text{CF}_3\text{SO}_3$ or BF_4] affords the analogous species $[\text{W}\{\text{C}(\text{OMe})\text{C}=\text{C}(\text{H})\text{Ph}\}(\text{S}_2\text{CNR}_2)(\text{CO})(\text{dppe})]$. In seeking to extend this chemistry we have examined the deprotonation of the bis(alkyne) halogeno complexes $[\text{MoBr}(\eta^2\text{-MeC}_2\text{R})_2(\eta\text{-C}_5\text{H}_5)]$ ($\text{R} = \text{Ph}$ **4** or Me **5**), also the $\eta^2(4e)$ -alkyne/ $\eta^2(2e)$ -alkene cation $[\text{Mo}(\eta^2\text{-MeC}_2\text{Ph})(\text{dppe})(\eta\text{-C}_5\text{H}_5)][\text{BF}_4]$ **6** ($\text{dppe} = o$ -diphenylphosphinostyrene), and have discovered novel chemistry, which is described in detail⁴ in this paper.

Results and Discussion

In the light of our earlier observations and the complementary studies of Templeton and co-workers,³ it was thought that the deprotonation of bis(alkyne) halogeno complexes of the type $[\text{MoX}(\eta^2\text{-MeC}_2\text{R})_2(\eta\text{-C}_5\text{H}_5)]$ ⁵ would result in the formation of the $\eta^2(3e)$ -allenyl/ $\eta^2(4e)$ -alkyne substituted complex $[\text{Mo}\{\text{C}(\text{R})\text{C}=\text{CH}_2\}(\eta^2\text{-MeC}_2\text{R})(\eta\text{-C}_5\text{H}_5)]$. When $\text{Li}[\text{N}(\text{SiMe}_3)_2]$ was added (-78 to $+25^\circ\text{C}$) to a stirred solution of $[\text{MoBr}(\eta^2\text{-MeC}_2\text{Ph})_2(\eta\text{-C}_5\text{H}_5)]$ **4** in tetrahydrofuran (thf) there was a change from yellow to red. Work-up by extraction into hexane followed by recrystallisation from toluene-hexane afforded (65% yield) dark red air-sensitive crystals of **7**. Similarly, reaction of $[\text{MoBr}(\eta^2\text{-MeC}_2\text{Me})_2(\eta\text{-C}_5\text{H}_5)]$ **5** with $\text{Li}[\text{N}(\text{SiMe}_3)_2]$ afforded the low-melting pink solid **8**. Elemental analysis of **7** and a mass spectrum of **8** both showed that a molecule of HBr had indeed been eliminated. Examination of the ^1H NMR spectra revealed that in comparison with the halogeno complexes **4** and **5** there was one less methyl group present, indicating that the new complexes **7** and **8** had the molecular formula $[\text{Mo}(\text{C}_3\text{H}_2\text{R})(\eta^2\text{-MeC}_2\text{R})(\eta\text{-C}_5\text{H}_5)]$. The NMR spectra confirmed the presence of a co-ordinated alkyne, the ^1H spectrum of **8** showing a singlet at δ 2.50 due to the equivalent methyl groups of a rotating $\eta^2(4e)$ -bonded but-2-yne, collapsing at low temperature to singlets at δ 2.27 and 2.15. The $^{13}\text{C}\{^1\text{H}\}$ spectra of **7** and **8** exhibited the expected⁶ low-field signals attributable to the contact carbons

* Reactions of Co-ordinated Ligands. Part 59.¹

Supplementary data available: see Instructions for Authors, *J. Chem. Soc., Dalton Trans.*, 1995, Issue 1, pp. xxv-xxx.

of four-electron donor alkynes, but the spectra did not show low-field resonances (δ ca. 250) characteristic of the α -carbon of an $\eta^2(3e)$ -allenyl fragment. A further indication that **7** and **8** did not contain an $\eta^2(3e)$ -allenyl ligand was the observation that although the ^1H spectra showed the presence of a $\text{C}=\text{CH}^b\text{H}^b$ system, the $J(\text{H}^a\text{H}^b)$ coupling constants [**7** (10.8), **8** (9.5 Hz)] were greater than that expected (ca. 2–3 Hz) for an uncoordinated $\text{C}=\text{CH}^a\text{H}^b$ group.

In order to establish the nature of the dehydrohalogenation reaction and the structural identity of these complexes it was therefore clearly important to carry out a single-crystal X-ray diffraction study, and after some difficulty a crystal of **7** was obtained from toluene–hexane. The resulting structure is shown in Fig. 1, fractional coordinates and selected bond lengths and angles being listed in Tables 1 and 2 respectively. This confirmed that the molecule contains a molybdenum atom to which are co-ordinated an η^5 -cyclopentadienyl group, an η^2 -bonded MeC_2Ph and a phenyl substituted $\sigma, \eta^2(3e)$ -prop-2-ynyl fragment, the last two ligands lying in planes essentially parallel to that of the η^5 - C_5H_5 .

The presence of a prop-2-ynyl (σ, η^2 - C_3H_3) ligand within the molecule is particularly interesting, because complexes containing it have recently been described. Thus, the unsubstituted cation $[\text{Mo}\{\sigma, \eta^2(3e)\text{-CH}_2\text{C}_2\text{H}\}(\text{CO})_2(\eta^6\text{-C}_6\text{Me}_6)]^+[\text{BF}_4]^-$ was prepared⁷ by photolysis of $[\text{Mo}(\text{CO})_3(\eta^6\text{-C}_6\text{Me}_6)]$ and prop-2-ynyl alcohol in the presence of HBF_4 ; hydride abstraction by $[\text{Ph}_3\text{C}][\text{PF}_6]$ from the two-electron donor but-2-yne complex $[\text{Re}(\eta^2\text{-MeC}_2\text{Me})(\text{CO})_2(\eta\text{-C}_5\text{Me}_5)]$ has been shown⁸ to give

$[\text{Re}\{\sigma, \eta^2(3e)\text{-CH}_2\text{C}_2\text{Me}\}(\text{CO})_2(\eta\text{-C}_5\text{Me}_5)]^+[\text{PF}_6]^-$; reaction of $[\text{ZrCl}_2(\eta\text{-C}_5\text{H}_5)_2]$ and $[\text{Zr}(\text{Me})\text{Cl}(\eta\text{-C}_5\text{H}_5)_2]$ with the Grignard reagent $\text{PhC}_2\text{CH}_2\text{MgBr}$ affords $[\text{Zr}\{\sigma\text{-CH}_2\text{C}_2\text{Ph}\}(\sigma, \eta^2\text{-}(3e)\text{-CH}_2\text{C}_2\text{Ph})(\eta\text{-C}_5\text{H}_5)_2]$ and $[\text{ZrMe}\{\sigma, \eta^2(3e)\text{-CH}_2\text{C}_2\text{Ph}\}(\eta\text{-C}_5\text{H}_5)_2]$ respectively;⁹ and finally and most recently the cation $[\text{Pt}\{\sigma, \eta^2(3e)\text{-CH}_2\text{C}_2\text{H}\}(\text{PPh}_3)_2]^+[\text{PF}_6]^-$ has been shown¹⁰ to be formed on reaction of *cis*- $[\text{Pt}\{\sigma(1e)\text{-CH}_2\text{C}_2\text{H}\}\text{-Cl}(\text{PPh}_3)_2]$ with TIPF_6 . The preparation of **7** and **8** establishes, therefore, a new synthetic pathway to these ligands and constitutes the first synthesis of a three-electron σ, η^2 -prop-2-ynyl complex by deprotonation of a four-electron donor η^2 -alkyne ligand.

The cationic molybdenum complex $[\text{Mo}\{\sigma, \eta^2(3e)\text{-CH}_2\text{-C}_2\text{H}\}(\text{CO})_2(\eta^6\text{-C}_6\text{Me}_6)]^+[\text{BF}_4]^-$ and the zirconium complex $[\text{ZrMe}\{\sigma, \eta^2(3e)\text{-CH}_2\text{C}_2\text{Ph}\}(\eta\text{-C}_5\text{H}_5)_2]$ have both been structurally characterised by single-crystal X-ray crystallography, and it was clearly interesting to compare the bond parameters of the prop-2-ynyl ligand reported for these two complexes with those found for **7**. As is evident from an examination of Table 3 there are major variations in the $\text{C}(1)\text{--C}(2)\text{--C}(3)$ angle, and in the $\text{C}(1)$, $\text{C}(2)$ and $\text{C}(3)$ carbon–carbon bond lengths, suggesting that the $\sigma, \eta^2(3e)\text{-C}_3\text{H}_3$ ligand can adopt different bonding modes. In order, therefore, to examine the nature of the metal C_3H_3 bonding, and its relationship to the structures observed for the three complexes, a comparative standard extended-Hückel molecular orbital (EHMO) study was carried out as implemented in the CACAO2 program using the published molecular parameters and with the simplification that the phenyl substituent in the zirconium complex is replaced by a hydrogen atom.¹¹

The isolated prop-2-ynyl fragments in all three complexes display similar geometries in the sense that they have shorter $\text{C}(2)\text{--C}(3)$ distances than $\text{C}(1)\text{--C}(2)$ distances and $\text{C}(1)\text{--C}(2)\text{--C}(3)$ angles around 150° . The fragment molecular orbitals (FMOs) for the three prop-2-ynyl units are very similar and are displayed schematically in Fig. 2. Focusing on the C–C π -type orbitals, the intraligand bonding appears at first sight to

Table 1 Fractional atomic coordinates for complex **7**

Atom	x	y	z
Mo	0.848 36(5)	0.835 09(4)	0.214 59(2)
C(1)	0.727 2(10)	1.012 7(7)	0.174 3(4)
C(2)	0.748 1(10)	1.037 6(7)	0.240 9(4)
C(3)	0.651 6(10)	0.958 1(7)	0.275 2(4)
C(4)	0.571 9(8)	0.878 5(8)	0.233 3(4)
C(5)	0.615 0(9)	0.914 6(7)	0.168 6(4)
C(6)	0.948 0(7)	0.720 1(5)	0.146 3(2)
C(7)	0.798 7(6)	0.685 3(6)	0.158 3(2)
C(8)	0.670 9(8)	0.601 4(7)	0.134 0(3)
C(9)	1.080 3(6)	0.683 0(6)	0.102 8(2)
C(10)	1.184 3(7)	0.773 3(6)	0.076 3(3)
C(11)	1.301 1(8)	0.739 3(6)	0.030 9(3)
C(12)	1.317 5(8)	0.612 5(7)	0.012 6(3)
C(13)	1.216 6(8)	0.525 3(6)	0.038 2(3)
C(14)	1.097 8(8)	0.558 1(6)	0.084 0(3)
C(15)	0.921 0(7)	0.773 0(5)	0.307 1(3)
C(16)	1.043 8(6)	0.832 8(6)	0.284 8(2)
C(17)	1.105 9(8)	0.904 2(7)	0.233 2(3)
C(18)	0.865 2(7)	0.712 3(5)	0.366 5(2)
C(19)	0.960 0(9)	0.709 8(6)	0.421 7(3)
C(20)	0.905 2(10)	0.657 5(7)	0.479 0(3)
C(21)	0.753 0(12)	0.607 9(7)	0.481 0(3)
C(22)	0.653 7(11)	0.606 6(7)	0.427 1(3)
C(23)	0.709 8(8)	0.661 3(7)	0.369 9(3)

Table 2 Selected bond lengths (Å) and angles ($^\circ$) for complex **7**

Mo–C(1)	2.296(7)	Mo–C(2)	2.375(7)
Mo–C(3)	2.430(7)	Mo–C(4)	2.355(6)
Mo–C(5)	2.305(7)	Mo–C(6)	2.039(5)
Mo–C(7)	2.016(6)	Mo–C(15)	2.105(5)
Mo–C(16)	2.164(5)	Mo–C(17)	2.278(6)
C(6)–C(7)	1.308(8)	C(6)–C(9)	1.466(7)
C(7)–C(8)	1.470(8)	C(15)–C(16)	1.281(8)
C(15)–C(18)	1.459(8)	C(16)–C(17)	1.404(9)
C(7)–Mo–C(6)	37.6(2)	C(15)–Mo–C(6)	108.8(2)
C(15)–Mo–C(7)	109.2(2)	C(16)–Mo–C(6)	98.9(2)
C(16)–Mo–C(7)	121.7(2)	C(16)–Mo–C(15)	34.9(2)

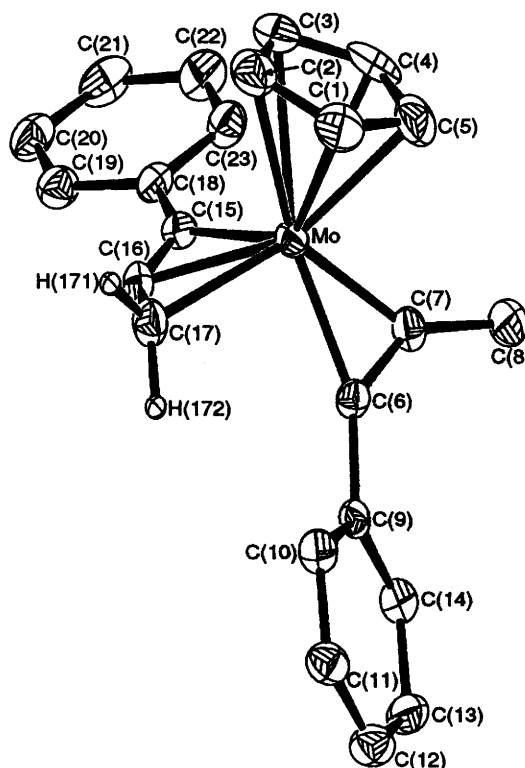
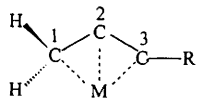
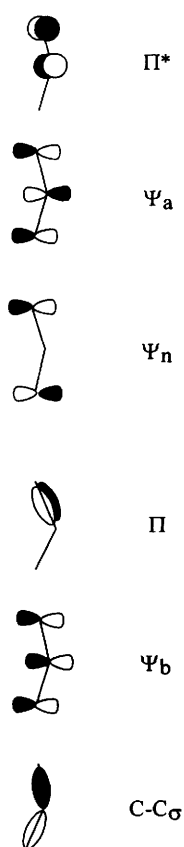


Fig. 1 Molecular structure of $[\text{Mo}\{\sigma, \eta^2(3e)\text{-CH}_2\text{C}_2\text{PPh}\}\{\eta^2(4e)\text{-MeC}_2\text{Ph}\}(\eta\text{-C}_5\text{H}_5)]$ **7**

Table 3 Bond parameters of $\sigma,\eta^2(3e)$ -prop-2-ynyl complexes


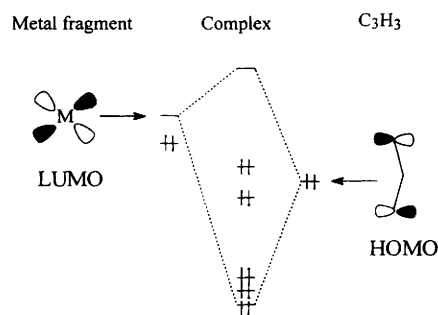
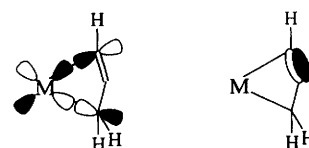
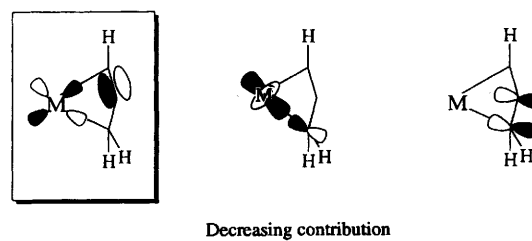
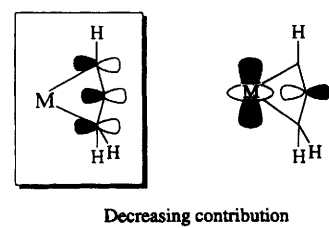
Complex	R	Bond length/Å					Angle/° C(1)–C(2)–C(3)
		C(1)–C(2)	C(2)–C(3)	M–C(1)	M–C(2)	M–C(3)	
7 [Mo(σ,η^2 -CH ₂ C ₂ R)(η^2 -MeC ₂ R)(η -C ₅ H ₅)]	Ph	1.404(9)	1.281(8)*	2.278(6)	2.164(5)	2.105(5)	146.1(6)
[Mo(σ,η^2 -CH ₂ C ₂ R)(CO) ₂ (η^6 -C ₆ Me ₆)] [BF ₄]	H	1.380(4)	1.236(4)	2.340(3)	2.282(3)	2.319(3)	150.9(3)
[ZrMe(σ,η^2 -CH ₂ C ₂ R)(η -C ₅ H ₅) ₂]	Ph	1.344(5)	1.259(4)	2.658(4)	2.438(3)	2.361(3)	155.4(3)

* By comparison the $\eta^2(4e)$ -bonded MeC₂Ph ligand present in complex 7 has a C(6)–C(7) separation of 1.308(8) Å.

**Fig. 2** Orbitals of $\sigma,\eta^2(3e)$ -prop-2-ynyl

resemble allyl-like functions, which extend over the whole carbon framework, and an additional π bond between C(2) and C(3) perpendicular to the 'allyl' functions. However, the analogy with the η^3 -allyl ligand cannot be taken too far since the relevant MOs lie in the plane of the prop-2-ynyl fragment while in an η^3 -allyl fragment these functions are perpendicular to the ligand plane.

In all three complexes the M–C₃H₃ interaction is dominated by a single interaction between the ligand HOMO (highest occupied MO) and the metal fragment LUMO (lowest unoccupied MO) as shown schematically in Fig. 3. There is also strong evidence for a π bond lying perpendicular to the ligand plane between C(2) and C(3). These common features of the bonding are shown in Fig. 4. Thus, the C₃H₃ ligand binds mainly through its terminal carbons C(1) and C(3), while the C(2)–C(3) π bond does not interact significantly with the metal fragment. In addition to these there are a number of secondary orbital interactions, which vary from complex to complex. These interactions are shown in Figs. 5–7. The most important

**Fig. 3** Metal and C₃H₃ orbital interactions**Fig. 4** Principal $\sigma,\eta^2(3e)$ -prop-2-ynyl molecular orbital interactions**Fig. 5** Additional orbital interactions in the complex [ZrMe($\sigma,\eta^2(3e)$ -CH₂C₂Ph)(η^6 -C₆Me₆)] [BF₄]**Fig. 6** Additional orbital interactions in the complex [Mo($\sigma,\eta^2(3e)$ -CH₂C₂H)(CO)₂(η^6 -C₆Me₆)] [BF₄]

one for each complex is highlighted and gives an insight into the differences between the bonding modes. Both complex 7 and the zirconium complex contain a very asymmetrically bonded C₃H₃ ligand with the M–C(1) distance significantly longer than the M–C(3) contact. The orbital interactions shown in Figs. 5 and 7 illustrate how C(3) is rather more firmly held than C(1). In contrast, the extra orbital interaction for the cation of

$[\text{Mo}\{\sigma, \eta^2(3\text{e})\text{-CH}_2\text{C}_2\text{H}\}(\text{CO})_2(\eta^6\text{-C}_6\text{Me}_6)][\text{BF}_4]$ is concentrated in a C_3H_3 function, which extends more or less equally over the whole ligand, and therefore tends to favour a rather more symmetrical binding. Hence, the $\text{Mo-C}(1)$ and $\text{Mo-C}(3)$ distances in this case are almost identical.

Although these secondary interactions rationalise why with the zirconium complex and with **7** the C_3H_3 ligand is asymmetrically bonded, they also highlight the variations in the $\text{M-C}_3\text{H}_3$ bonding. Valence-bond representations provide an alternative view and Fig. 8 shows schematic representations of the formal valence-bond canonical structures for $\text{M-C}_3\text{H}_3$ binding. Indeed, it is interesting that the structures of such complexes have previously⁷⁻⁹ been described in terms of one or other of the outer two forms, however the present EHMO

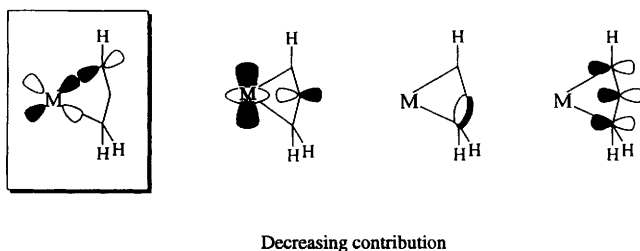


Fig. 7 Additional orbital interactions in the complex $[\text{Mo}\{\sigma, \eta^2(3\text{e})\text{-CH}_2\text{C}_2\text{PPh}\}\{\eta^2(4\text{e})\text{-MeC}_2\text{PPh}\}(\eta\text{-C}_5\text{H}_5)]$ **7**

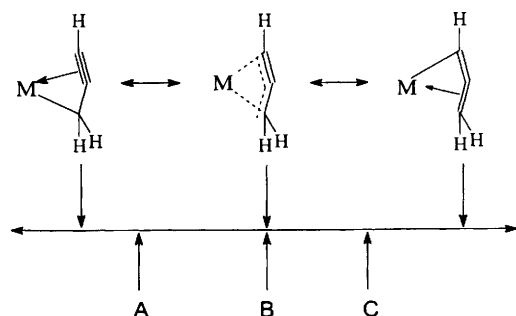
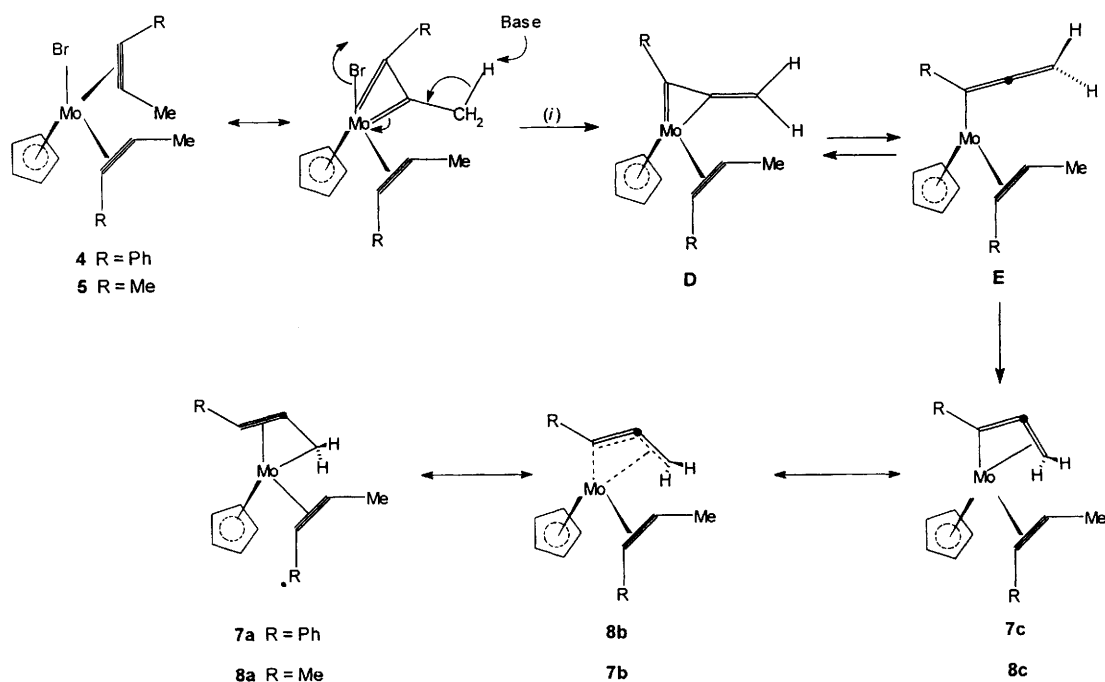


Fig. 8 Overview of canonical forms, where A = zirconium complex, B = cationic molybdenum complex, C = **7**



Scheme 1 (i) $\text{Li}[\text{N}(\text{SiMe}_3)_2]$, thf, $-\text{LiBr}$, $-\text{NH}(\text{SiMe}_3)_2$

calculations suggest that a third canonical structure is also relevant and this is shown in the centre of Fig. 8. Taking all of the theoretical data together, it is clear that the cation of $[\text{Mo}\{\sigma, \eta^2(3\text{e})\text{-CH}_2\text{C}_2\text{H}\}(\text{CO})_2(\eta^6\text{-C}_6\text{Me}_6)][\text{BF}_4]$ conforms to this representation, whilst the zirconium complex and **7** lie at the two extremes. Hence, despite the qualitatively similar asymmetric bonding mode for the latter two species, the bonding is better described by different canonical forms.

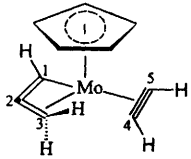
With regard to the formation of complexes **7** and **8** it was noted earlier that deprotonation of the halogeno complexes **4** and **5** was expected to result in the formation of an $\eta^2(3\text{e})$ -allenyl/ $\eta^2(4\text{e})$ -alkyne-substituted complex. It is suggested that this actually occurs, but the kinetically controlled product **D** (Scheme 1) then transforms under thermodynamic control *via* a ring-opening process [$\eta^2(3\text{e})$ -allenyl \rightarrow $\eta^1(1\text{e})$ -allenyl] into the $\eta^1(1\text{e})$ -allenyl-substituted complex **E**, thus providing access to the $18\text{e } \sigma, \eta^2(3\text{e})$ -prop-2-ynyl/ $\eta^2(4\text{e})$ -alkyne-substituted complexes **7** and **8**.

The complexes **7** and **8** are obviously also of interest from the standpoint of reactivity and because of their mode of formation, *i.e.* deprotonation, their reactivity towards protonic acids HA was examined. Treatment (-78 to $+25^\circ\text{C}$) of **7** with trifluoroacetic acid in dichloromethane solution resulted in a change from red to yellow, and work-up by recrystallisation afforded the bis(alkyne) complex $[\text{Mo}(\text{O}_2\text{CCF}_3)(\eta^2\text{-MeC}_2\text{Ph})_2(\eta\text{-C}_5\text{H}_5)]$ **9** characterised by elemental analysis and NMR spectroscopy. A similar reaction between **8** and $\text{CF}_3\text{CO}_2\text{H}$ resulted in the formation of $[\text{Mo}(\text{O}_2\text{CCF}_3)(\eta^2\text{-MeC}_2\text{Me})_2(\eta\text{-C}_5\text{H}_5)]$ **10**, which was similarly characterised. These reactions are especially interesting because a Z-shaped $\sigma, \eta^2(3\text{e})$ -prop-2-ynyl fragment is transformed on protonation into a U-shaped η^2 -alkyne ligand. As a first step towards understanding this process it was clearly important to examine the charge distribution within molecules of the type represented by **7** and **8**, because it was a reasonable assumption that the protonation reaction is charge controlled.

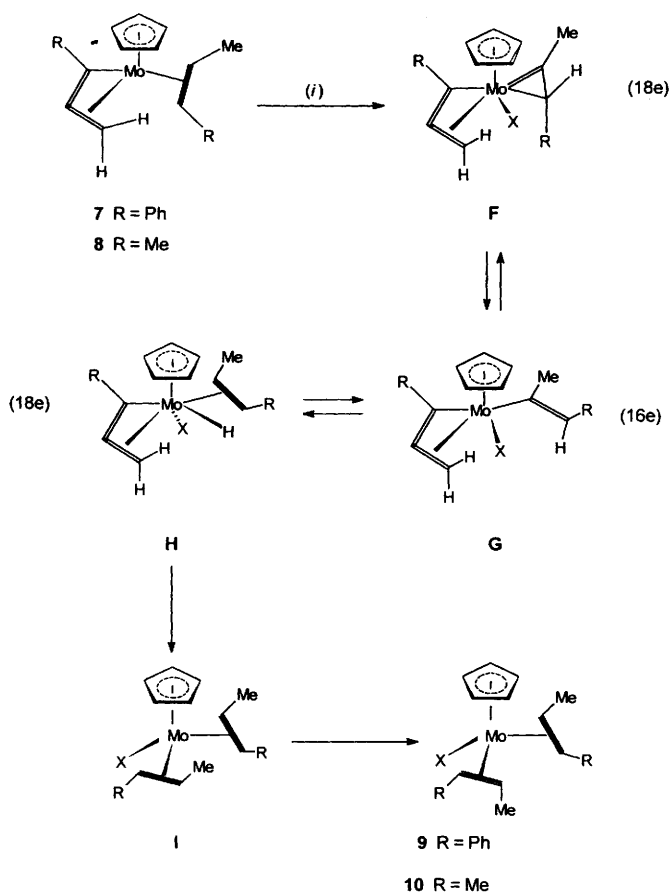
An EHMO calculation using the bond parameters established for complex **7** gave the charge distribution listed in Table 4, indicating that direct protonation of the prop-2-ynyl methylene group, *i.e.* C(3), is unlikely, and that if the C_3H_3 fragment is actually the site of an initial charge-controlled attack by a proton then this is more likely to occur on the opposite end [C(1)] of the prop-2-ynyl ligand. This

would, however, lead to the formation of the $\eta^2(2e)$ -allene/ $\eta^2(4e)$ -alkyne-substituted species $[\text{Mo}\{\text{OC}(\text{O})\text{CF}_3\}_2\{\eta^2\text{-CH}(\text{Ph})\text{C}=\text{CH}_2\}(\eta^2\text{-MeC}_2\text{Ph})(\eta\text{-C}_5\text{H}_5)]$, a type of complex which would be expected to be stable and not likely to rearrange *via* an H-shift process into the isolated product **9**. This mechanistic difficulty is avoided if, as illustrated in Scheme 2, and in agreement with the calculations (Table 4), protonation is postulated to occur on the alkyne contact carbon *cis* to the prop-2-ynyl methylene group thus affording the $\eta^2(3e)$ -vinyl-substituted intermediate **F**. There is in fact precedent for the formation of an $\eta^2(3e)$ -vinyl ligand by the protonation of an $\eta^2(4e)$ -alkyne,¹² and there is also a precedent¹³ for the transformation of an $\eta^2(3e)$ - into an $\eta^1(1e)$ -vinyl as is required by the step **F** \rightarrow **G**. A β -hydrogen elimination reaction **G** \rightarrow **H**, followed by migration of the MoH hydrogen onto the methylene end of the prop-2-ynyl ligand, thus provides access to

Table 4 Charge distribution in $[\text{Mo}(\sigma, \eta^2\text{-CH}_2\text{C}_2\text{H})(\eta^2\text{-HC}_2\text{H})(\eta\text{-C}_5\text{H}_5)]$



Atom	Charge
Mo	0.739
C(1)	-0.316
C(2)	0.102
C(3)	-0.165
C(4)	-0.304
C(5)	-0.240



the conformationally unstable η^2 -U-alkyne/ η^2 -Z-alkyne-substituted species **I**, an obvious precursor of the isolated product **9**.

Having shown in our earlier studies² that deprotonation of the cation of $[\text{Mo}(\eta^2\text{-PhC}_2\text{CH}_2\text{Ph})\{\text{P}(\text{OMe})_3\}_2(\eta\text{-C}_5\text{H}_5)][\text{BF}_4]$ affords isomeric $\eta^2(3e)$ -allenyl complexes, whereas dehydrohalogenation of the bis(alkyne) complexes $[\text{MoBr}(\eta^2\text{-MeC}_2\text{R})_2(\eta\text{-C}_5\text{H}_5)]$ gives the $\sigma, \eta^2(3e)$ -prop-2-ynyl/ $\eta^2(4e)$ -alkyne-substituted complexes **7** and **8**, it was obviously interesting and important to extend our studies and examine the deprotonation of an η^2 -alkene/ $\eta^2(4e)$ -alkyne-substituted molybdenum complex, and discover which of these two different types of product were formed. We had previously¹⁴ established that the reaction of $[\text{Mo}(\text{CO})(\eta^2\text{-MeC}_2\text{Me})_2(\eta\text{-C}_5\text{H}_5)][\text{BF}_4]$ with *o*-diphenylphosphinostyrene (dpps) affords the η^2 -alkene/ η^2 -alkyne-substituted complex $[\text{Mo}(\eta^2\text{-MeC}_2\text{Me})_2(\text{dpps})(\eta\text{-C}_5\text{H}_5)][\text{BF}_4]$ and, therefore, the reaction of this cation with $\text{Li}[\text{N}(\text{SiMe}_3)_2]$ was examined. However, although a reaction occurred attempts to isolate a stable product were unsuccessful. Attention was then turned to the phenyl substituted analogue, $[\text{Mo}(\eta^2\text{-MeC}_2\text{Ph})_2(\text{dpps})(\eta\text{-C}_5\text{H}_5)][\text{BF}_4]$ **6**. This was formed in high yield by reaction of $[\text{Mo}(\text{CO})(\eta^2\text{-MeC}_2\text{Ph})_2(\eta\text{-C}_5\text{H}_5)][\text{BF}_4]$ with dpps in refluxing dichloromethane and was structurally characterised by NMR spectroscopy and by single-crystal X-ray crystallography. The crystallographic study established, as is shown in Fig. 9 (fractional coordinates and selected bond lengths and angles in Tables 5 and 6), that the cation adopts a similar structure to that found¹⁴ in the but-2-yne complex. As in the parent but-2-yne complex, the C–C vectors of the co-ordinated alkene (dpps) and $\eta^2\text{-MeC}_2\text{Ph}$ ligand lie essentially parallel to the Mo–P axis, and as shown by the NMR spectra there is only one isomer formed, *i.e.* the one with the methyl substituent on the $\eta^2(4e)$ -alkyne *cis* to the phosphorus ligand.

Treatment (-78 to $+25$ °C) of a suspension of complex **6** in thf with 1 molar equivalent of $\text{Li}[\text{N}(\text{SiMe}_3)_2]$ led on stirring to rapid dissolution of the solid and a change from red to yellow. Column chromatography (alumina) of the reaction mixture and elution with a hexane–dichloromethane mixture afforded yellow crystals of **11** (70% yield). Examination of the NMR spectra (see Experimental section) of the neutral product revealed that as expected a proton had been abstracted from the methyl substituent of the $\eta^2(4e)$ -bonded alkyne, however, resonances characteristic of either a $\sigma, \eta^2(3e)$ -prop-2-ynyl or an $\eta^2(3e)$ -allenyl ligand were absent suggesting that an unexpected reaction had occurred. This was confirmed by a single-crystal X-ray diffraction study, which showed (Fig. 10, fractional coordinates and selected bond lengths and angles in Tables 7 and 8) that the product of the deprotonation reaction was, surprisingly, a d^4 molybdenum η^5 -pentadienyl complex where

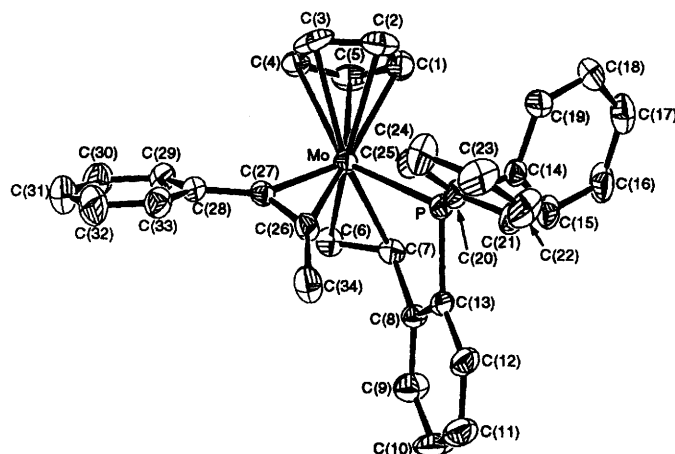


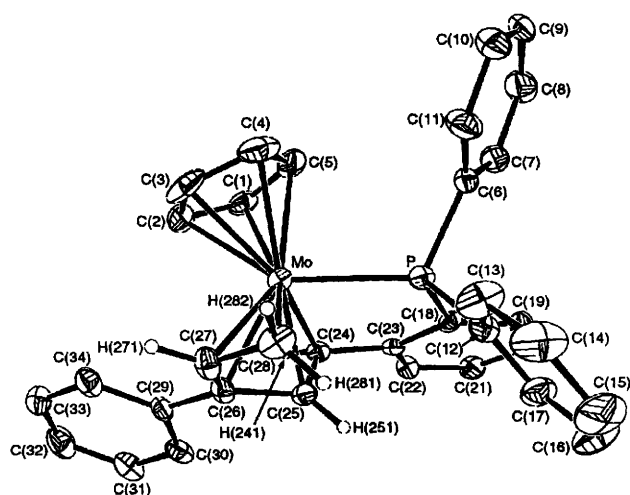
Fig. 9 Molecular structure of $[\text{Mo}(\eta^2\text{-MeC}_2\text{Ph})(\text{dpps})(\eta\text{-C}_5\text{H}_5)]^+[\text{BF}_4]^-$ **6**

Table 5 Fractional atomic coordinates for complex **6**

Atom	x	y	z	Atom	x	y	z
Mo	0.347 8(1)	0.187 32(4)	0.186 00(3)	C(20)	0.110 4(5)	0.225 6(5)	0.051 7(4)
P	0.187 8(1)	0.138 3(1)	0.110 0(1)	C(21)	0.016 2(6)	0.194 5(6)	0.012 8(4)
C(1)	0.258 6(7)	0.174 7(8)	0.300 5(4)	C(22)	-0.042 8(7)	0.259 7(8)	-0.032 4(5)
C(2)	0.245 6(8)	0.267 0(8)	0.270 9(4)	C(23)	-0.008 3(8)	0.356 7(8)	-0.039 4(5)
C(3)	0.344 6(11)	0.315 4(7)	0.273 4(4)	C(24)	0.083 4(6)	0.388 7(6)	-0.001 5(5)
C(4)	0.416 9(7)	0.246 3(9)	0.305 0(4)	C(25)	0.042 2(5)	0.322 0(6)	0.044 8(3)
C(5)	0.362 0(8)	0.160 8(6)	0.321 8(3)	C(26)	0.388 7(5)	0.234 0(5)	0.081 9(3)
C(6)	0.451 5(6)	0.049 7(5)	0.191 6(4)	C(27)	0.462 7(5)	0.258 7(5)	0.133 5(3)
C(7)	0.349 0(6)	0.020 0(5)	0.167 1(3)	C(28)	0.564 8(5)	0.307 7(5)	0.139 1(3)
C(8)	0.317 6(5)	-0.009 9(5)	0.086 4(4)	C(29)	0.642 5(6)	0.280 1(5)	0.193 7(4)
C(9)	0.362 7(6)	-0.088 6(6)	0.050 5(4)	C(30)	0.742 1(6)	0.321 0(7)	0.194 6(5)
C(10)	0.328 1(7)	-0.112 7(7)	-0.023 3(5)	C(31)	0.766 4(7)	0.388 5(7)	0.140 5(6)
C(11)	0.247 8(7)	-0.060 9(7)	-0.060 7(5)	C(32)	0.692 1(8)	0.418 1(7)	0.086 6(5)
C(12)	0.200 7(6)	0.016 4(6)	-0.025 5(4)	C(33)	0.591 3(6)	0.378 6(5)	0.085 4(4)
C(13)	0.234 6(5)	0.041 6(5)	0.049 2(3)	C(34)	0.377 6(6)	0.239 8(6)	-0.003 7(3)
C(14)	0.084 2(5)	0.077 9(5)	0.162 4(3)	B	0.321 5(9)	0.572 5(10)	0.136 8(7)
C(15)	0.078 5(5)	-0.023 9(5)	0.169 6(4)	F(1)	0.245 2(9)	0.520 5(9)	0.099 3(5)
C(16)	0.003 4(6)	-0.066 9(6)	0.213 3(5)	F(2)	0.415 2(7)	0.569 2(15)	0.112 0(6)
C(17)	-0.065 6(6)	-0.008 2(7)	0.252 0(5)	F(3)	0.279 8(12)	0.669 5(7)	0.136 8(5)
C(18)	-0.060 9(6)	0.093 4(7)	0.245 4(4)	F(4)	0.324 3(4)	0.549 8(5)	0.211 7(3)
C(19)	0.012 2(6)	0.035 9(5)	0.200 8(4)				

Table 6 Selected bond lengths (Å) and angles (°) for complex **6**

P–Mo	2.455(4)	C(1)–Mo	2.362(19)
C(2)–Mo	2.290(9)	C(3)–Mo	2.310(9)
C(4)–Mo	2.359(8)	C(5)–Mo	2.409(8)
C(6)–Mo	2.269(9)	C(7)–Mo	2.278(9)
C(26)–Mo	2.026(8)	C(27)–Mo	2.005(8)
C(14)–P	1.830(8)	C(20)–P	1.811(8)
C(7)–C(6)	1.401(10)	C(7)–C(8)	1.506(10)
C(27)–C(26)	1.311(9)	C(34)–C(26)	1.503(10)
C(28)–C(27)	1.447(9)		
C(6)–C(7)–Mo	71.7(5)	C(8)–C(7)–Mo	113.5(5)
C(8)–C(7)–C(6)	124.0(7)	C(9)–C(8)–C(7)	122.9(7)
C(27)–C(26)–Mo	70.2(5)	C(34)–C(26)–Mo	154.6(5)
C(34)–C(26)–C(27)	134.7(6)	C(26)–C(27)–Mo	71.9(5)
C(28)–C(27)–Mo	148.4(5)	C(28)–C(27)–C(26)	139.7(6)

**Fig. 10** Molecular structure of $[\text{Mo}\{\eta^2, \eta^3(\text{Se})\text{-CH}_2\text{CHC(Ph)CH=CHC}_6\text{H}_4\text{PPh}_2\text{-o}\}(\eta\text{-C}_5\text{H}_5)]$ **11**

the pentadienyl ligand adopts the relatively rare η^5 -S(sickle) conformation and is wrapped around the molybdenum centre resulting in a dihedral angle of 122° for C(27)–C(26)–C(25)–C(24). The C(24)–C(25) vector is twisted out of the C(25)C(26)C(27)C(28) plane by 53° , which results in the effective bonding of all five carbon atoms of the pentadienyl ligand to the molybdenum atom with Mo–C distances in the

range 2.139(8)–2.292(8) Å. The distances C(26)–C(27) 1.403(12) and C(27)–C(28) 1.416(13) Å show slight asymmetry in the bonding of the allylic fragment, however the most significant feature is the bond length C(25)–C(26) of 1.484(11) Å consistent with there being little interaction between the two π -systems.

There is no precedent for such a carbon–carbon bond forming reaction, and although there has recently^{15–24} been considerable interest in the chemistry of pentadienyl complexes this represents a new synthetic approach to these C_5 ligands. In considering how the η^5 -S-pentadienyl complex **11** is formed it is reasonable to assume that the first step involves the loss of a proton from the co-ordinated alkyne methyl group resulting in the formation of the $\eta^2(3\text{e})$ -allenyl-substituted complex **J** (Scheme 3). Since **J** contains a metal to carbon double bond and a co-ordinated alkene with a relative *cis* configuration it might at first sight be assumed that these ligands would react as in the metathesis reaction to form a metallocyclobutane.^{25–27} Such a step is, however, unlikely because the alkene ligand is not free to rotate and cannot therefore be orientated parallel to the metal–carbene bond, a geometrical pre-requisite* for the formation of a metallocyclobutane. This suggests that instead **J** must first rearrange into the $\sigma, \eta^2(3\text{e})$ -prop-2-ynyl/ η^2 -alkene-substituted species **K** before transforming into **L** via an insertion reaction. In order to convert **L** into the isolated product **11** it is necessary for the co-ordinated allene to dissociate from the metal centre so that following C–C bond rotation the *cis*-coplanar geometry needed for a β -hydrogen elimination reaction **M** \rightarrow **N** can be attained. Insertion of the η^2 -co-ordinated allene into the Mo–H bond, *i.e.* **N** \rightarrow **O**, followed by rotation about the C–C bond **O** \rightarrow **P** then provides access to **11** with the observed stereochemistry.

The formation of the pentadienyl complex **11** was an unexpected bonus in that such a molecule might be expected to have an interesting reaction chemistry. Owing to our interest throughout this investigation in deprotonation and protonation reactions we investigated the reactivity of **11** towards proton sources. An EHMO calculation based on the bond parameters derived from the X-ray crystallographic study on **11** established

* Recently²⁸ in a study of the reaction of the iridium complex $[\text{Ir}(\text{=CH}_2)\{\text{N}(\text{SiMe}_2\text{CH}_2\text{PPh}_2)_2\}]$ with alkenes, evidence has been obtained for a pathway involving perpendicular approach of the alkene to the Ir=CH₂ bond. This type of reaction is, however, facilitated by the electron-withdrawing substituents on the alkene, *i.e.* can be depicted as a Michael addition.

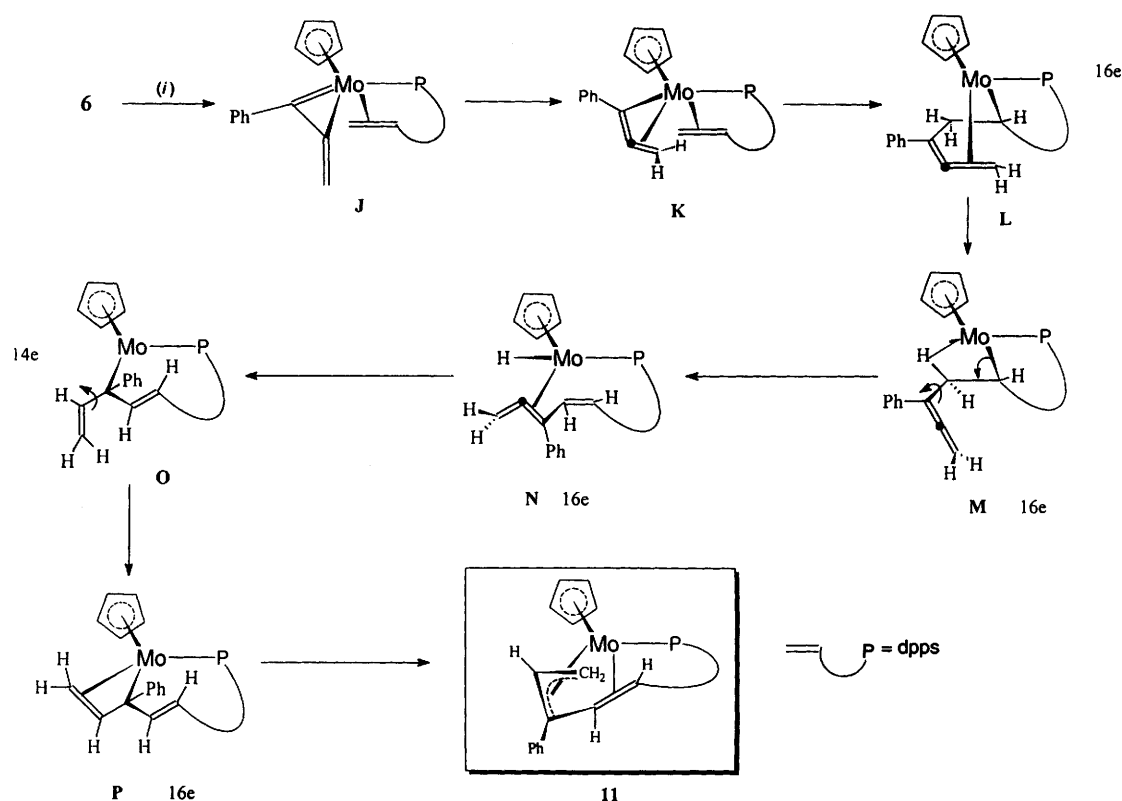
Scheme 3 (i) $\text{Li}[\text{N}(\text{SiMe}_3)_2]$, thf, -78 to $+25$ °C

Table 7 Fractional atomic coordinates for complex 11

Atom	x	y	z	Atom	x	y	z
Mo	0.240 31(7)	0.203 12(3)	0.133 98(3)	C(20)	0.358 0(9)	0.034 0(4)	-0.051 6(5)
P	0.182 7(2)	0.109 5(1)	0.104 8(1)	C(21)	0.446 3(8)	0.074 2(4)	-0.068 0(4)
C(1)	0.188 2(9)	0.266 1(4)	0.050 1(5)	C(22)	0.456 9(8)	0.121 4(3)	-0.030 0(4)
C(2)	0.211 0(9)	0.295 3(4)	0.106 9(5)	C(23)	0.381 0(7)	0.128 8(3)	0.024 9(4)
C(3)	0.120 8(12)	0.279 6(5)	0.155 3(5)	C(24)	0.398 2(7)	0.177 5(4)	0.069 4(4)
C(4)	0.044 5(9)	0.240 7(5)	0.124 4(7)	C(25)	0.420 2(7)	0.165 6(3)	0.137 8(5)
C(5)	0.087 3(11)	0.231 9(4)	0.060 8(6)	C(26)	0.421 9(8)	0.215 6(3)	0.179 5(4)
C(6)	0.025 8(5)	0.101 6(2)	0.069 3(3)	C(27)	0.334 2(9)	0.215 6(4)	0.230 6(4)
C(7)	0.010 6(5)	0.094 6(2)	0.001 8(3)	C(28)	0.254 4(11)	0.169 8(4)	0.239 1(4)
C(8)	-0.108 6(5)	0.093 2(2)	-0.025 3(3)	C(29)	0.509 0(5)	0.263 0(2)	0.166 2(3)
C(9)	-0.212 6(5)	0.099 0(2)	0.015 1(3)	C(30)	0.617 6(5)	0.254 1(2)	0.130 2(3)
C(10)	-0.197 3(5)	0.106 0(2)	0.082 7(3)	C(31)	0.699 6(5)	0.297 5(2)	0.118 7(3)
C(11)	-0.078 1(5)	0.107 4(2)	0.109 8(3)	C(32)	0.673 1(5)	0.349 8(2)	0.143 1(3)
C(12)	0.187 8(6)	0.052 3(3)	0.164 7(3)	C(33)	0.564 5(5)	0.358 7(2)	0.179 1(3)
C(13)	0.108 8(6)	0.054 2(3)	0.219 0(3)	C(34)	0.482 4(5)	0.315 3(2)	0.190 6(3)
C(14)	0.108 3(6)	0.011 0(3)	0.264 2(3)	H(241)	0.440 8(58)	0.207 9(20)	0.047 6(32)
C(15)	0.186 8(6)	-0.034 0(3)	0.255 0(3)	H(251)	0.438 4(62)	0.128 6(14)	0.153 5(32)
C(16)	0.265 9(6)	-0.035 9(3)	0.200 7(3)	H(271)	0.314 2(64)	0.248 6(17)	0.255 5(28)
C(17)	0.266 4(6)	0.007 3(3)	0.155 5(3)	H(281)	0.288 4(60)	0.132 4(14)	0.243 3(34)
C(18)	0.289 0(7)	0.089 6(3)	0.039 1(4)	H(282)	0.183 6(44)	0.173 9(28)	0.268 7(28)
C(19)	0.280 5(7)	0.041 5(3)	0.001 4(4)				

the electron-density distribution listed in Table 9. This indicated that charge-controlled protonation should be directed to C(28) (crystallographic numbering) of the pentadienyl chain resulting in the formation of a co-ordinatively unsaturated cationic *trans*- η^4 -1,3-diene complex.^{29,30} In order to stabilise such a product it was expected that an additional two-electron donor ligand such as carbon monoxide would be required.

Treatment (-78 to $+25$ °C) of a dichloromethane solution of complex 11 with 1 molar equivalent of $\text{HBF}_4 \cdot \text{Et}_2\text{O}$ in the presence of a stream of carbon monoxide led to a rapid change from yellow to orange. Addition of diethyl ether afforded orange crystals of the cationic complex 12. Surprisingly, the IR spectrum of 12 showed no evidence for the presence of a co-

ordinated carbon monoxide ligand, and when it was found that 11 was reformed in excellent yield by treating 12 with the base $\text{Li}[\text{N}(\text{SiMe}_3)_2]$ it became apparent that the product of the protonation reaction $11 \rightarrow 12$ probably derived stability from an agostic³¹ $\text{Mo}(\mu\text{-H})\text{C}$ interaction. This was confirmed by an examination of the ambient-temperature ^1H NMR spectrum of 12, which showed a high-field broad singlet resonance at $\delta -2.0$ attributable to three hydrogens, suggesting the presence of an agostic methyl group, which in solution at room temperature undergoes 'in-place rotation'. This was supported by the observation that in the low-temperature (-80 °C) ^1H NMR spectrum this high-field signal was replaced by three resonances at δ 2.33, -1.13 and -7.56 , each integrating for one hydrogen.

A single-crystal X-ray diffraction study with the cationic complex **12** established the solid-state structure illustrated in Fig. 11, fractional coordinates and selected bond lengths and angles being listed in Tables 10 and 11 respectively. The presence of an agostic methyl group was confirmed by the bond parameters: Mo–H(281) 1.915(48), Mo–C(28) 2.437(6) Å, C(28)–Mo–H(281) 24.3(13)°. A structural feature of special interest involved the carbon atoms C(24), C(25), C(26) and C(27), which adopt a twisted, non-planar arrangement with a dihedral angle of 123° very similar to that observed (122°) in the parent complex **11**. The central carbon atoms C(25) and C(26) are slightly closer to the molybdenum centre [Mo–C(25) 2.151(7), Mo–C(26) 2.232(7) Å] than the terminal carbons C(24) and C(27) [Mo–C(24) 2.290(7), Mo–C(27) 2.246(5) Å].

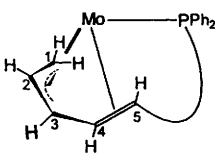
Interestingly, the carbon–carbon bond lengths C(26)–C(27), C(25)–C(26) and C(24)–C(25) are approximately equivalent

(Table 12), which is consistent with the current bonding rationale suggested by Legzdins and co-workers for $[\text{Mo}(\text{NO})(\eta^4\text{-trans-C}_4\text{H}_6)(\eta\text{-C}_5\text{H}_5)]^{32}$ and $[\text{Mo}(\text{NO})(\eta^4\text{-trans-C}_5\text{H}_8)(\eta\text{-C}_5\text{Me}_5)]^{33}$ complexes. This is in marked contrast to the $\eta^4\text{-trans-1,3-diene}$ complex $[\text{Zr}(\eta^4\text{-trans-PhCH=CHCH=CHPh})(\eta\text{-C}_5\text{H}_5)_2]$, which exhibits short–long–short carbon–carbon bond lengths characteristic of a diene.³⁴ It is reasonable to suggest, therefore, that **12** is a cationic $\eta^4\text{-trans-1,3-diene}$ complex (see Scheme 4). Furthermore, as in the $[\text{Mo}(\text{NO})(\text{trans-diene})(\eta\text{-C}_5\text{H}_5)]$ complexes, **12** shows no

Table 8 Selected bond lengths (Å) and angles (°) for complex **11**

Mo–P	2.433(3)	Mo–C(24)	2.235(8)
Mo–C(25)	2.139(8)	Mo–C(26)	2.182(8)
Mo–C(27)	2.231(9)	Mo–C(28)	2.292(8)
C(23)–C(24)	1.502(11)	C(24)–C(25)	1.439(11)
C(25)–C(26)	1.484(11)	C(26)–C(27)	1.403(12)
C(26)–C(29)	1.509(10)	C(27)–C(28)	1.416(13)
C(24)–C(23)–C(18)	119.9(7)	C(25)–C(24)–C(23)	116.4(8)
C(26)–C(25)–C(24)	113.0(7)	C(27)–C(26)–C(25)	114.6(8)
C(29)–C(26)–C(25)	122.1(7)	C(29)–C(26)–C(27)	123.3(7)
C(28)–C(27)–C(26)	119.8(8)		

Table 9 Charge distribution in $[\text{Mo}(\eta^2, \eta^3\text{-CH}_2\text{CHCHCH=CHC}_6\text{H}_4\text{-PPh}_2\text{-}o)(\eta\text{-C}_5\text{H}_5)]$



Atom	Charge
Mo	0.197
C(1)	–0.266
C(2)	0.013
C(3)	–0.096
C(4)	–0.134
C(5)	–0.168

Table 10 Fractional atomic coordinates for complex **12**

Atom	x	y	z
Mo	0.248 85(3)	0.162 60(3)	0.127 48(2)
P	0.264 7(1)	0.183 0(1)	0.269 1(1)
C(1)	0.366 3(5)	0.146 3(5)	0.064 9(4)
C(2)	0.421 7(5)	0.169 1(7)	0.142 5(5)
C(3)	0.392 6(6)	0.270 9(7)	0.157 3(4)
C(4)	0.323 3(6)	0.307 9(5)	0.089 5(5)
C(5)	0.306 9(5)	0.232 0(5)	0.032 0(3)
C(6)	0.370 8(4)	0.261 3(4)	0.333 4(3)
C(7)	0.468 7(4)	0.217 4(5)	0.360 4(4)
C(8)	0.551 4(5)	0.272 2(5)	0.407 7(4)
C(9)	0.539 6(5)	0.371 6(5)	0.427 6(4)
C(10)	0.444 1(5)	0.417 5(5)	0.398 6(4)
C(11)	0.358 9(5)	0.361 6(4)	0.350 8(3)
C(12)	0.145 7(4)	0.229 1(4)	0.283 0(3)
C(13)	0.105 2(4)	0.323 8(5)	0.254 4(3)
C(14)	0.010 2(5)	0.355 9(5)	0.259 4(4)
C(15)	–0.045 1(5)	0.293 6(6)	0.291 2(4)
C(16)	–0.006 1(5)	0.199 5(7)	0.320 0(4)
C(17)	0.088 6(5)	0.165 5(5)	0.315 6(4)
C(18)	0.295 5(4)	0.056 5(4)	0.314 2(3)
C(19)	0.320 9(5)	0.039 2(5)	0.394 3(3)

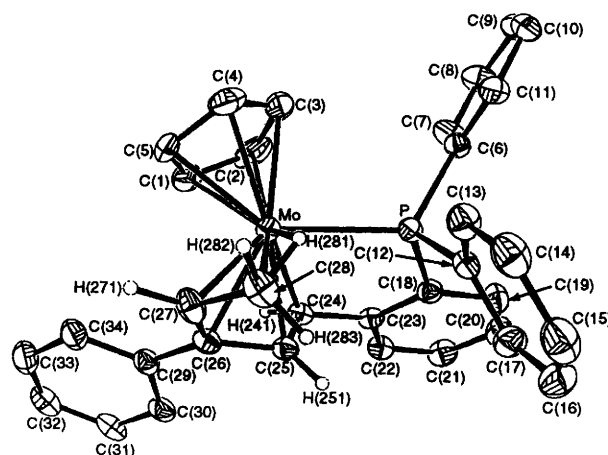


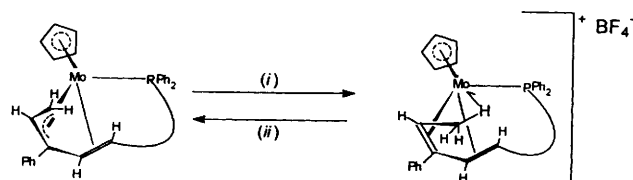
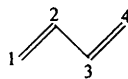
Fig. 11 Molecular structure of $[\text{Mo}\{\eta^2, \eta^2(\mu_{\text{Mo,C-H}})\text{MeCHC(Ph)-CH=CHC}_6\text{H}_4\text{PPh}_2\text{-}o\}(\eta\text{-C}_5\text{H}_5)]$ **12**

Table 11 Selected bond lengths (Å) and angles (°) for complex **12**

P–Mo	2.505(4)	C(24)–Mo	2.290(7)
C(25)–Mo	2.151(7)	C(26)–Mo	2.232(7)
C(27)–Mo	2.246(5)	C(28)–Mo	2.437(6)
H(281)–Mo	1.915(48)	C(24)–C(23)	1.478(8)
C(25)–C(24)	1.448(7)	C(26)–C(25)	1.442(8)
C(27)–C(26)	1.403(9)	C(29)–C(26)	1.493(9)
C(28)–C(27)	1.496(11)		
C(24)–C(23)–C(18)	119.3(5)	C(25)–C(24)–C(23)	118.4(6)
C(26)–C(25)–C(24)	113.9(6)	C(27)–C(26)–C(25)	114.9(6)
C(28)–C(27)–C(26)	120.5(6)	C(28)–H(281)–Mo	106.9(37)

Table 12 Bond lengths (Å) for η^4 -*trans*-diene complexes

Complex	C(1)–C(2)	C(2)–C(3)	C(3)–C(4)
12	1.403(9)	1.442(8)	1.448(7)
[Mo(NO)(η^4 - <i>trans</i> -C ₅ H ₈)(η -C ₅ Me ₅)]	1.386(8)	1.422(8)	1.405(8)
[Mo(NO)(η^4 - <i>trans</i> -C ₄ H ₆ (η -C ₅ H ₅)]	1.401(4)	1.408(4)	1.418(4)
[Zr(η^4 - <i>trans</i> -PhHC=CHCH=CHPh)(η -C ₅ H ₅) ₂]	1.40	1.48	1.40

**Scheme 4** (i) HBF₄·Et₂O, CH₂Cl₂; (ii) Li[N(SiMe₃)₂], thf

evidence of isomerisation of the bound diene to the *cis* form as occurs in the [Zr(η^4 -*trans*-diene)(η -C₅H₅)₂] complexes.

Attempts to displace the Mo(μ -H)C interaction with a carbon monoxide ligand failed, however preliminary experiments³⁵ have shown that the reaction of complex **12** with LiI or MeCN does result in the displacement of the agostic interaction and that *trans* to *cis* isomerisation of the 1,3-diene moiety occurs. This implies that the 1,3-diene present in **12** is 'locked' in a *trans* conformation by the agostic interaction. Such an effect has not been observed previously.

Experimental

The ¹H, ¹³C-{¹H}, ³¹P-{¹H} and ¹⁹F NMR spectra were recorded on JEOL GX270 and EX400 spectrometers. Data are given for room-temperature measurements unless otherwise stated. Chemical shifts are referenced relative to tetramethylsilane, external H₃PO₄ and CCl₃F respectively. Infrared spectra were recorded on a Nicolet 580P FT-IR spectrometer. All reactions were carried out in Schlenk tubes under atmospheres of dry oxygen-free nitrogen, using freshly distilled and degassed solvents. Column chromatography was performed using BDH alumina, Brockman activity II unless otherwise stated, as the solid support. The complexes [MoBr(η^2 -MeC₂R)₂(η -C₅H₅)] R = Ph **4** or Me **5** were prepared by published procedures.

Preparation of [Mo{ σ , η^2 (3e)-CH₂C₂Ph}(η^2 -MeC₂Ph)(η -C₅H₅)] **7.**—A solution of Li[N(SiMe₃)₂] (1.0 mmol, 1 mol dm⁻³ solution in hexane) was added (–78 °C) dropwise with stirring to [MoBr(η^2 -MeC₂Ph)₂(η -C₅H₅)] **4** (0.47 g, 1.0 mmol) dissolved in tetrahydrofuran (15 cm³). On warming to room temperature the solution changed from yellow to red. After 45 min at room temperature the volatiles were removed *in vacuo*, and the residue was extracted with hexane and filtered through Celite (4 × 25 cm). Removal of the hexane and recrystallisation (0 °C) from toluene–hexane (1 : 1) afforded dark red crystals of complex **7** (0.25 g, 65%) (Found: C, 70.2; H, 5.1. Calc. for C₂₃H₂₀Mo: C, 70.4; H, 5.1%). NMR(C₆D₆): ¹H, δ 8.03–6.99 (m, 10 H, Ph), 5.01 [d, 1 H, H^a, *J*(H^aH^b) 10.8], 4.88 (s, 5 H, C₅H₅), 3.90 [d, 1 H, H^b, *J*(H^aH^b) 10.8] and 2.42 (s, 3 H, MeC₂Ph); ¹³C-{¹H}, δ 208.4 (C \equiv C), 197.0 (C \equiv C), 142.3 (=C=), 140.8–126.8 (Ph), 124.8 (CPh), 93.6 (C₅H₅), 41.6 (CH₂) [¹H-

coupled ¹³C spectrum, dd, CH^aH^b, *J*(CH^a) 158.6, *J*(CH^b) 165.3 Hz] and 18.9 (Me).

Preparation of [Mo{ σ , η^2 (3e)-CH₂C₂Me}(η^2 -MeC₂Me)(η -C₅H₅)] **8.**—Similarly, the reaction (–78 °C) of [MoBr(η^2 -MeC₂Me)₂(η -C₅H₅)] **5** (0.4 g, 1.5 mmol) with Li[N(SiMe₃)₂] (1.5 mmol, 1 mol dm⁻³ solution in hexane) in thf (15 cm³) led on warming to room temperature to a change from yellow to deep pink. Work-up by the above procedure gave the pink oil **8** (0.23 g, 75%). NMR(C₆D₆CD₃): ¹H, δ 4.95 (s, 5 H, C₅H₅), 4.77 [dq, 1 H, H^a, *J*(H^aH^b) 9.5, *J*(HMe) 2.2], 3.85 [dq, 1 H, H^b, *J*(H^aH^b) 9.5, *J*(HMe) 2.2], 2.50 (s, 6 H, MeC₂Me) (collapsed to singlets at δ 2.27 and 2.15, $\Delta G^\ddagger_T = 34 \pm 2$ kJ mol⁻¹, *T*_c 198 K and 2.47 [t, 3 H, CMe, *J*(HMe) 2.2]; ¹³C-{¹H}, δ 199.7 (C \equiv C), 133.6 (=C=), 112.4 (CMe), 93.3 (C₅H₅), 38.6 (CH₂) [¹H-coupled ¹³C spectrum, dd, CH^aH^b, *J*(CH^a) 156.4, *J*(CH^b) 163.0 Hz], 20.4 (CMe) and 19.0 (Me). Mass spectrum: *m/z* 268 (*M*⁺) and 214 (*M*⁺ – MeC₂Me).

Reactions of Trifluoroacetic Acid.—With complex **7**. Addition (–78 to +25 °C) of CF₃CO₂H (29 μ l, 0.37 mmol) to a solution of complex **7** (0.17 g, 0.30 mmol) in dichloromethane (10 cm³) resulted in a change from red to yellow. After 1.5 h the volatiles were removed *in vacuo* and the resulting yellow solid recrystallised (–20 °C) from toluene–hexane to give yellow crystals of [Mo(O₂CCF₃)(η^2 -MeC₂Ph)₂(η -C₅H₅)] **9** (0.10 g, 60%) (Found: C, 63.8; H, 3.7. Calc. for C₃₁H₂₁F₃MoO₂: C, 64.1; H, 3.6%). NMR(CD₂Cl₂): ¹H, δ 7.80–7.00 (m, 10 H, Ph), 5.65 (s, 5 H, C₅H₅) and 3.2–2.4 (br s, 6 H, Me); ¹³C-{¹H}, δ 186.8 (br s, C \equiv C), 168.2 (br s, C \equiv C), 163.3 [q, CCF₃, *J*(CF) 37.5], 130.1–128.4 (Ph), 116.3 [q, CF₃, *J*(CF) 292 Hz], 102.9 (C₅H₅) and 21.5 (Me); ¹⁹F, δ –75.6 (s).

With complex 8. Similarly, reaction (–78 to +25 °C) of CF₃CO₂H (39 μ l, 0.50 mmol) with complex **8** (0.14 g, 0.50 mmol) gave on recrystallisation (–20 °C) from toluene–hexane yellow crystals of [Mo(O₂CCF₃)(η^2 -MeC₂Me)₂(η -C₅H₅)] **10** (0.89 g, 55%) (Found: C, 46.9; H, 4.5. Calc. for C₁₅H₁₇F₃MoO₂: C, 46.8; H, 4.4%). NMR(C₆D₆): ¹H, δ 5.06 (s, 5 H, C₅H₅) and 2.37 (s, 12 H, MeC \equiv C); ¹³C-{¹H}, δ 183.4 (br s, C \equiv C), 169.8 (br s, C \equiv C), 164.1 [q, CCF₃, *J*(CF) 35.0], 117.8 [q, CF₃, *J*(CF) 292.3], 101.5 (C₅H₅) and 20.9 (br s, Me); ¹⁹F, δ –74.2 (s).

Preparation of [Mo(η^2 -MeC₂Ph)(dppe)(η -C₅H₅)] [BF₄][–] **6.**—A solution of [Mo(η^2 -MeC₂Ph)₂(CO)(η -C₅H₅)] [BF₄][–] (0.51 g, 1 mmol) and dppe (0.29 g, 1 mmol) in dichloromethane (20 cm³) was refluxed for 24 h. On cooling and addition of diethyl ether (20 cm³) a red solid was precipitated. Recrystallisation (0 °C) from CH₂Cl₂–Et₂O afforded red crystals of complex **6** (0.64 g, 98%) (Found: C, 60.4; H, 4.5. Calc. for C₃₄H₃₀BF₄MoP₂: C, 59.6; H, 4.5%). NMR: ¹H (CDCl₃), δ 8.0–7.0 (m, 14 H, aryl), 5.52 (s, 5 H, C₅H₅), 5.33 (s, CH₂Cl₂), 4.41 (m, 1 H, H^c), 2.86 [br d, 1 H, H^b, *J*(H^bH^c) 8.6], 1.75 (s, 3 H, Me) and 1.00 [br d, 1 H, H^a, *J*(H^aH^c) 14.1]; ¹³C-{¹H} (CD₂Cl₂), δ 229.6 [d, \equiv CPh, *J*(CP) 22.6], 220.5 [d, \equiv CMe, *J*(CP) 5.5], 150.4–127.9 (Ph), 100.4 (C₅H₅), 61.7 (C⁵), 35.6 (C²) and 20.5 [d, \equiv CMe, *J*(CP) 8.1 Hz]; ³¹P-{¹H} (CDCl₃), δ 80.2 (s). Mass spectrum: *m/z* 567 (*M*⁺) and 87 (*M*[–]).

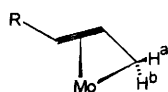
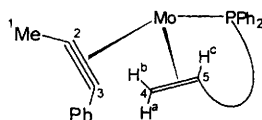


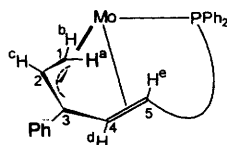
Table 13 Structure analyses for compounds **6**, **7**, **11** and **12**^a

	6	7	11	12
Formula	C ₃₄ H ₃₀ BF ₄ MoP	C ₂₃ H ₂₀ Mo	C ₃₄ H ₂₉ MoP	C ₃₄ H ₃₀ BF ₄ MoP·0.46CH ₂ Cl ₂
<i>M</i>	652.3	392.4	564.5	691.0
Crystal system	Monoclinic	Orthorhombic	Orthorhombic	Monoclinic
Space group	<i>P</i> 2 ₁ / <i>c</i>	<i>P</i> 2 ₁ 2 ₁ 2 ₁	<i>Pbca</i>	<i>P</i> 2 ₁ / <i>c</i>
<i>a</i> /Å	12.636(1)	8.2346(7)	10.748(1)	13.705(2)
<i>b</i> /Å	13.467(2)	10.667(2)	24.315(4)	12.995(2)
<i>c</i> /Å	17.559(2)	20.604(2)	20.348(3)	18.040(3)
β/°	93.02(1)	—	—	109.49(1)
<i>U</i> /Å ³	2983.9	1809.8	5317.7	3028.7
<i>Z</i>	4	4	8	4
<i>D</i> _c /g cm ⁻³	1.39	1.44	1.41	1.52
<i>F</i> (000)	1268	780	2320	1496
μ(Mo-Kα)/cm ⁻¹	5.20	6.39	5.60	5.46
Crystal dimensions/mm	0.2 × 0.2 × 0.1	0.2 × 0.2 × 0.1	0.3 × 0.3 × 0.07	0.3 × 0.3 × 0.2
No. parameters refined	393	227	306	356, 48 ^b
Max shift/e.s.d.	0.004	0.033	0.010	0.050
Total data	5149	1859	4651	5115
Unique data	2539	1442	1764	3441
<i>R</i> , <i>R'</i>	0.0474, 0.0363	0.0267, 0.0292	0.0456, 0.0378	0.0454, 0.0489
Weighting expression, <i>w</i>	2.7450/[σ ² (<i>F</i>) + 0.000 136(<i>F</i>) ²]	0.3668/[σ ² (<i>F</i>) + 0.002 592(<i>F</i>) ²]	2.7485/[σ ² (<i>F</i>) + 0.000 466(<i>F</i>) ²]	2.1567/[σ ² (<i>F</i>) + 0.000 830(<i>F</i>) ²]
Maximum, minimum residual densities in difference map/e Å ⁻³	+0.24, -0.16	+0.15, -0.20	+0.19, -0.30	+0.51, -0.39

^a Details in common: *T* = 293 K; λ(Mo-Kα) 0.709 30 Å; 2θ range 4–48°; ω–2θ scans; *R* = Σ|Δ|/Σ|*F*_o|; *R'* = (Σ*w*Δ²/Σ*wF*_o²)^{1/2}; Δ = *F*_o – *F*_c. ^b Cation and anion refined in separate blocks respectively.

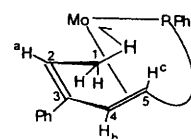


Deprotonation of Complex 6.—Lithium bis(trimethylsilyl)amide (0.9 cm³ of 1 mol dm⁻³ solution in thf, 0.9 mmol) was added at –78 °C to a stirred solution of complex **6** (0.50 g, 0.79 mmol) in tetrahydrofuran (20 cm³). After warming to room temperature and stirring for 1.5 h, the volatiles were removed *in vacuo* and then pre-absorbed on alumina. Column chromatography (alumina) and elution with hexane–dichloromethane (4:1) afforded a yellow band, which on collection and recrystallisation (0 °C) from toluene–hexane gave yellow crystals of [Mo{η²,η³(5e)-CH₂CHC(Ph)CH=CHC₆H₄PPh₂-o}(η-C₅H₅)] **11** (0.31 g, 70%) (Found: C, 71.3; H, 5.0. Calc. for C₃₄H₂₉MoP: C, 72.0; H, 5.2%). NMR (CD₂Cl₂): ¹H, δ 7.7–7.0 (m, 14 H, Ph), 5.28 [d, C₅H₅, 5 H, *J*(HP) 1.3], 4.62 [dd, 1 H, H^c, *J*(H^cH^b) 8.1, *J*(H^cH^a) 8.1], 3.76 [dd, 1 H, H^c, *J*(H^cH^d) 4.5, *J*(HP) 3.4], 2.31 [dd, 1 H, H^b, *J*(H^bH^c) 8.1, *J*(H^bH^a) 2.9], 0.44 [dd, 1 H, H^d, *J*(H^dH^c) 4.5, *J*(HP) 14.0] and –0.27 [ddd, 1 H, H^a, *J*(H^aH^c) 8.1, *J*(H^aH^b) 2.9, *J*(HP) 11.0]; ¹³C-{¹H}, δ 161.7–124.0 (Ph), 89.4 (C₅H₅), 77.9–77.5 (C^{3–5}), 55.7 (C²) and 37.0 [d, C¹, *J*(CP) 5.0 Hz]. Mass spectrum: *m/z* 566 (*M*⁺).



Protonation of Complex 11.—The adduct HBF₄·Et₂O (261 μl, 85% solution, 1.5 mmol) was added (–78 to +25 °C) to a stirred solution of complex **11** (0.74 g, 1.3 mmol) in dichloromethane (20 cm³). The reaction mixture was allowed to warm to room temperature and stirred for 2 h. The volatiles were removed *in vacuo* and the resulting solid recrystallised three times from CH₂Cl₂–Et₂O to afford orange crystals of **12** (0.57 g, 77%) (Found: C, 59.2; H, 4.5. Calc. for C₃₄H₃₀BF₄MoP·

0.5CH₂Cl₂: C, 59.6; H, 4.5%). NMR: ¹H [(CD₃)₂CO], δ 8.0–6.5 (m, 14 H, Ph), 5.65 [q, 1 H, H^b, *J*(H^bH^a) 6.4], 5.27 [d, 5 H, C₅H₅, *J*(HP) 1.1], 4.83 [dd, 1 H, H^c, *J*(H^cH^d) 5.5, *J*(HP) 3.3], 1.74 [dd, 1 H, H^d, *J*(H^dH^c) 5.5, *J*(HP) 9.4] and –2.0 (br s, 3 H, Me); ¹H (CD₂Cl₂, –80 °C), δ 2.33 (br s, 1 H), –1.13 (br s, 1 H) and –7.56 (br s, 1 H); ¹³C-{¹H} (CD₂Cl₂), δ 154.6–126.0 (Ph), 95.2 (C₅H₅), 90.5 (C³), 81.8 (C⁴ or C⁵), 75.9 (C⁴ or C⁵), 67.6 (C²) and 1.1 (C¹); ³¹P-{¹H} (CD₂Cl₂), δ 60.9 (s); ¹⁹F (CD₂Cl₂), δ –156.0. Mass spectrum: *m/z* 567 (*M*⁺) and 87 (*M*[–]).



Reaction of Complex 12 with Li[N(SiMe₃)₂].—Addition (–78 °C) of Li[N(SiMe₃)₂] (20 μl of 1 mol dm⁻³ solution in thf, 0.20 mmol) to a stirred solution of complex **12** (0.10 g, 0.18 mmol) in thf (10 cm³) resulted in a change from orange to yellow. Column chromatography afforded yellow crystals of **11** (0.82 g, 80%), identified by ¹H and ³¹P-{¹H} NMR spectroscopy.

Structure Determinations of Compounds 6, 7, 11 and 12.—Many of the details of the structural analyses are listed in Table 13. All X-ray diffraction measurements were made at ambient temperature using a CAD4 automatic four-circle diffractometer. Cell dimensions were universally determined from the setting-angle values of 25 reflections. All structures were solved using heavy-atom techniques and refined using the SHELX^{36,37} suite of programs. Compounds **6**, **7** and **11** were refined using full-matrix least squares, whereas **12** was refined in two-blocks (one for the cation and one for the anion). Hydrogen atoms were included at calculated positions in all cases except on carbons co-ordinated to the central molybdenum atom in each structure which were not part of a cyclopentadienyl ring.

In compound **6** the hydrogen atoms attached to C(6) and C(7) were located in the penultimate Fourier-difference map and refined at a fixed distance of 0.96 Å from the parent atoms.

Atoms H(171) and H(172) in **7** were similarly located and refined at a distance of 1.08 Å from C(17). The hydrogens associated with C(24)–C(28) in **11** and **12** were likewise identified and refined at distances of 0.98 and 0.94 Å from the relevant parent atoms in the respective structures.

The ORTEX³⁸ package was used to generate the molecular drawings in Figs. 1 and 9–11. Thermal ellipsoids are illustrated at the 30% probability level.

Additional material available from the Cambridge Crystallographic Data Centre comprises H-atom coordinates, thermal parameters and remaining bond lengths and angles.

Extended-Hückel Molecular Orbital Calculations.—Extended-Hückel MO calculations were performed using the CACAO2 program package of Mealli and Prosperio.¹¹ The structures employed the crystallographic coordinates of the three molecules [ZrMe{σ,η²(3e)-CH₂C₂Ph}(η-C₅H₅)₂], [Mo{σ,η²(3e)-CH₂C₂H}(CO)₂(η⁶-C₆Me₆)] [BF₄] and [Mo{σ,η²(3e)-CH₂C₂Ph}{η²(4e)-MeC₂Ph}(η-C₅H₅)} **7** with the simplification of all phenyl substituents being replaced by H atoms. All C–H distances were idealised to 1.10 Å. The EHMO parameters for molybdenum were as supplied with the CACAO program while those for zirconium were obtained from the literature.³⁹

Acknowledgements

We thank the SERC (EPSRC) for support and the award by Consiglio Nazionale delle Ricerche of a research fellowship (to C. C.). We also thank C. B. M. Nation for a preliminary experiment.

References

- Part 58, M. Bamber, G. C. Conole, R. J. Deeth, S. F. T. Froom and M. Green, *J. Chem. Soc., Dalton Trans.*, 1994, 3569.
- F. J. Feher, M. Green and R. A. Rodrigues, *J. Chem. Soc., Chem. Commun.*, 1987, 1206.
- A. S. Gamble, K. R. Birdwhistell and J. L. Templeton, *J. Am. Chem. Soc.*, 1990, **112**, 1818.
- C. Carfagna, M. Green, M. F. Mahon, S. Rumble and C. M. Woolhouse, *J. Chem. Soc., Chem. Commun.*, 1993, 879.
- G. C. Conole, M. Green, M. McPartlin, C. Reeve and C. M. Woolhouse, *J. Chem. Soc., Chem. Commun.*, 1988, 1310.
- J. L. Templeton, *Adv. Organomet. Chem.*, 1989, **29**, 1.
- M. I. Rybinskaya, *J. Organomet. Chem.*, 1990, **383**, 113; V. V. Krivykh, E. S. Taits, P. V. Petrovskil, Y. T. Struchkov and A. I. Yanovskii, *Mendeleev Commun.*, 1991, 103.
- C. P. Casey and C. S. Yi, *J. Am. Chem. Soc.*, 1992, **114**, 6597.
- P. W. Blosser, J. C. Gallucci and W. J. Wojcicki, *J. Am. Chem. Soc.*, 1993, **115**, 2994.
- J. Chen, T. Huang, G. Lee and Y. Wang, *J. Am. Chem. Soc.*, 1993, **115**, 1170.
- C. Mealli and D. Prosperio, *J. Chem. Educ.*, 1990, **67**, 399.
- G. C. Conole, M. Green, M. McPartlin, C. Reeve and C. M. Woolhouse, *J. Chem. Soc., Chem. Commun.*, 1988, 1313.
- S. R. Allen, R. G. Beevor, M. Green, N. C. Norman, A. G. Orpen and I. D. Williams, *J. Chem. Soc., Dalton Trans.*, 1985, 435.
- S. R. Allen, M. Green, G. Moran, A. G. Orpen and G. E. Taylor, *J. Chem. Soc., Dalton Trans.*, 1984, 441.
- S. R. Allen, M. Green, N. C. Norman, K. E. Paddick and A. G. Orpen, *J. Chem. Soc., Dalton Trans.*, 1983, 1625.
- L. Stahl, J. P. Hutchinson, D. R. Wilson and R. D. Ernst, *J. Am. Chem. Soc.*, 1985, **107**, 5016.
- G.-H. Lee, S.-M. Peng, T.-W. Lee and R.-S. Liu, *Organometallics*, 1986, **5**, 2378.
- G.-H. Lee, S.-M. Peng, S.-F. Lush, M.-Y. Liao and R.-S. Liu, *Organometallics*, 1987, **6**, 2094.
- M. Green, K. R. Nagle, C. M. Woolhouse and D. J. Williams, *J. Chem. Soc., Chem. Commun.*, 1987, 1793.
- T.-W. Lee and R.-S. Liu, *Organometallics*, 1988, **7**, 878.
- T. M. Siravec, T. J. Katz, M. Y. Chiang and G. X.-Q. Yang, *Organometallics*, 1989, **8**, 1620.
- J. W. Freeman, N. C. Hallinan, A. M. Arif, R. W. Gedridge, R. D. Ernst and F. Basolo, *J. Am. Chem. Soc.*, 1991, **113**, 6509.
- D. Seyforth, L. L. Anderson, F. Villafane and W. M. Davis, *J. Am. Chem. Soc.*, 1992, **114**, 4594.
- A. D. Horton and A. G. Orpen, *Organometallics*, 1992, **11**, 8.
- O. Eisenstein, R. Hoffmann and A. R. Rossi, *J. Am. Chem. Soc.*, 1981, **103**, 5582.
- J. Kress and J. A. Osborn, *Angew. Chem., Int. Ed. Engl.*, 1992, **31**, 1585.
- M. T. Youinou, J. Kress, J. Fischer, A. Aguero and J. A. Osborn, *J. Am. Chem. Soc.*, 1988, **110**, 1488.
- M. D. Fryzuk, X. Gao and S. J. Rettig, *J. Am. Chem. Soc.*, 1995, **117**, 3106.
- S. A. Benyunes, J. P. Day, M. Green, A. W. Al-Saadoon and T. L. Waring, *Angew. Chem., Int. Ed. Engl.*, 1990, **29**, 1416.
- S. A. Benyunes, A. Binelli, M. Green and M. J. Grimshire, *J. Chem. Soc., Dalton Trans.*, 1991, 895.
- M. Brookhart and M. L. H. Green, *J. Organomet. Chem.*, 1983, **250**, 395.
- A. D. Hunter, P. Legzdins, C. R. Nurse, F. W. B. Einstein and A. C. Willis, *J. Am. Chem. Soc.*, 1985, **107**, 1791.
- N. J. Christensen, P. Legzdins, F. W. B. Einstein and R. H. Jones, *Organometallics*, 1991, **10**, 3070.
- G. Erker, C. Krüger and G. Müller, *Adv. Organomet. Chem.*, 1985, **24**, 1; H. Yasuda, K. Tatsumi and A. Nakamura, *Acc. Chem. Res.*, 1985, **18**, 120 and refs. therein.
- M. Green, M. F. Mahon and J. M. McInnes, unpublished work.
- G. M. Sheldrick, SHELX 76, a computer program for crystal structure determination, University of Cambridge, 1976.
- G. M. Sheldrick, *Acta Crystallogr., Sect. A*, 1990, **46**, 467.
- P. McArdle, *J. Appl. Crystallogr.*, 1994, **27**, 438.
- Y. W. Aleyunas, N. C. Baenziger, P. K. Bradley and R. F. Jordan, *Organometallics*, 1994, **13**, 156.

Received 12th June 1995; Paper 5/03766B